Supplementary Material (ESI) for Energy & Environmental Science


# A high-power glucose/oxygen biofuel cell operating under quiescent conditions

Hideki Sakai[1], Takaaki Nakagawa[1], Yuichi Tokita[1], Tsuyonobu Hatazawa[1*], Tokuji Ikeda[2], Seiya Tsujimura[3] & Kenji Kano[3*]

[1]Advanced Materials Laboratories, Sony Corporation, Okata, Atsugi-shi, Kanagawa 243-0021, Japan, [2]Department of Biological Resources, Graduate School of Bioscience and Biotechnology, Fukui Prefectural University, Yoshida-gun, Fukui 910-1142, Japan, [3]Division of Applied Life Sciences, Graduate School of Agriculture, Kyoto University, Sakyo-ku, Kyoto 606-8502, Japan. Correspondence should be addressed to T.H. (Tsuyonobu.Hatazawa@jp.sony.com) and K.K. (kkano@kais.kyoto-u.ac.jp).

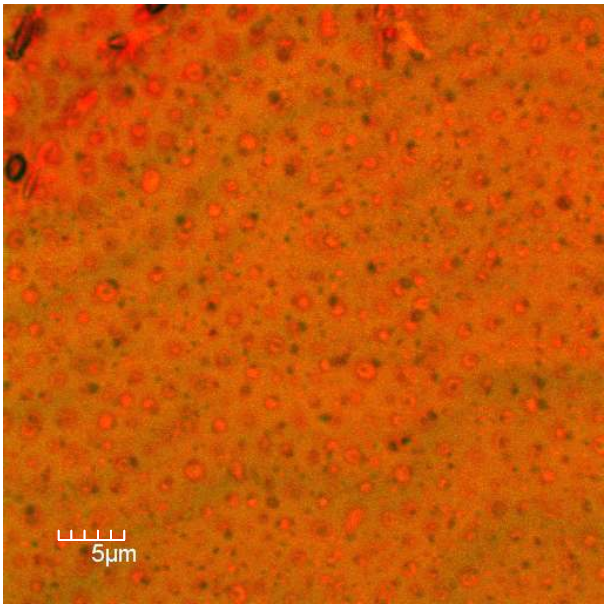


**Supplementary Figure 1** Confocal microscopic image of a GC-bioanode before electrochemical measurement. Orange color corresponds to the fluorescence of $VK_3$. Crater-like structures seem to be generated during the drying process. The thickness of the layer was evaluated from difference of the focal points between the top layer and the surface of the GC-electrode.

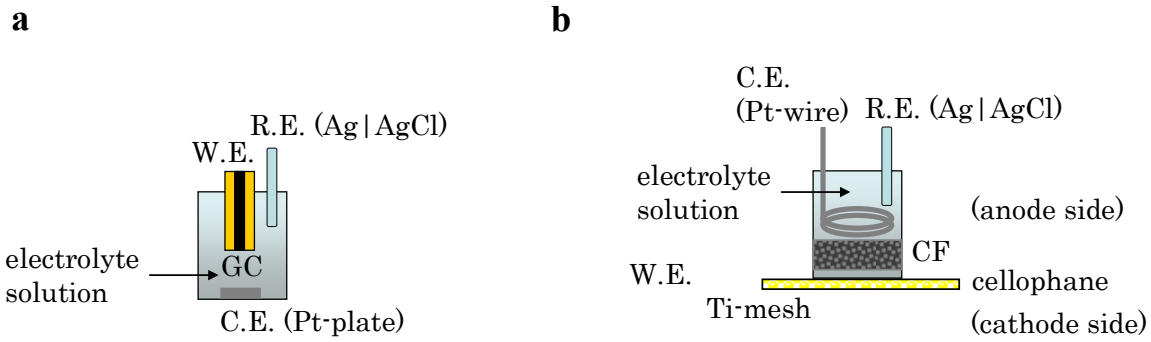


**Supplementary Figure 2** Schematic structure of the electrochemical cells for (**a**) GC-bioanode and (**b**) CF-bioanode. The volume of the solution is 1 ml for cell (**a**) and 3 ml for cell (**b**).

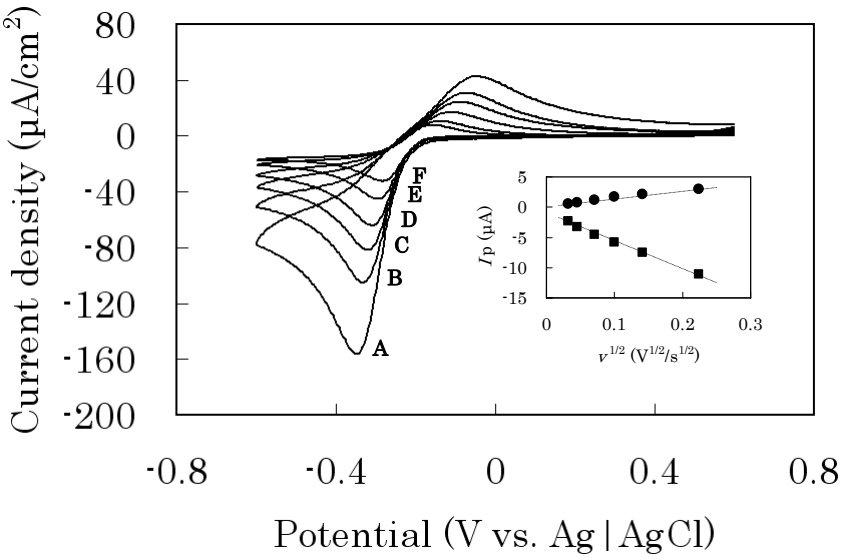


**Supplementary Figure 3** Voltammetric characterization of the GC-bioanode in the absence of glucose, using the electrochemical cell (**Supplementary Fig. 2a**). CV on a GC-bioanode at scan rate (*v*) of (A) 50, (B) 20, (C) 10, (D) 5, (E) 2, and (F) 1 mV/s (pH 7.0) are shown here. The inset shows the linear dependence of the peak current (*Ip*) on the square root of the scan rate (*v*). The peak separation was 126 mV at $v$ = 1 mV/s, which suggests a quasi-reversible electron transfer of $VK_3$ within the immobilized layer.

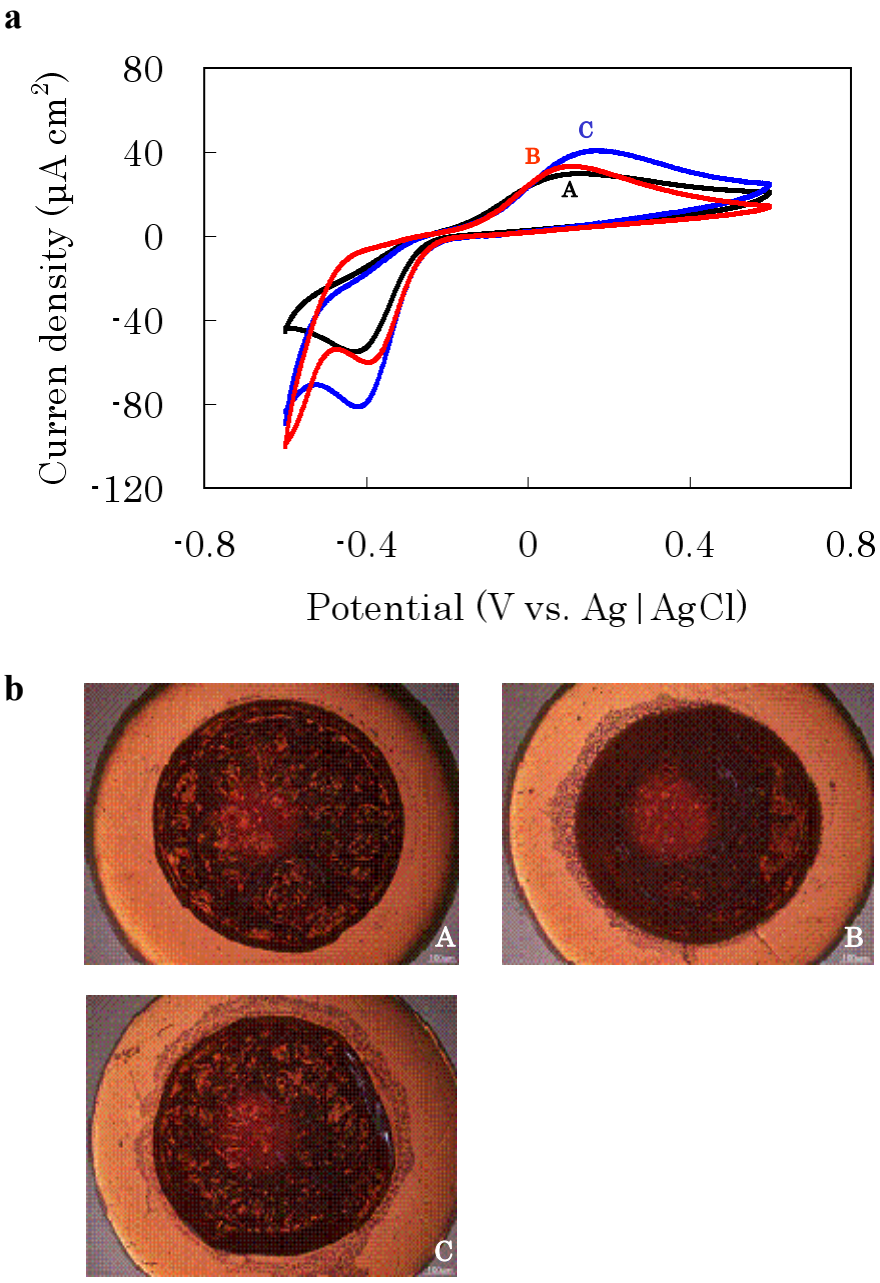


**Supplementary Figure 4** Stability evaluation of the immobilized layer of a GC-bioanode for the increased buffer concentration in the absence of glucose. (**a**) CV on a GC-bioanode at 10 mV/s in (A) 0.1, (B) 1.0, and (C) 2.0 M phosphate buffer solution (pH 7.0), using the electrochemical cell (**Supplementary Fig. 2a**). (**b**) Optical microscopic image of the enzyme/mediator-immobilized layer on the GC-electrode after CV in (A) 0.1, (B) 1.0, and (C) 2.0 M phosphate buffer solution (pH 7.0). The immobilized layer remained on the GC-electrode after CV in a high concentration buffer.

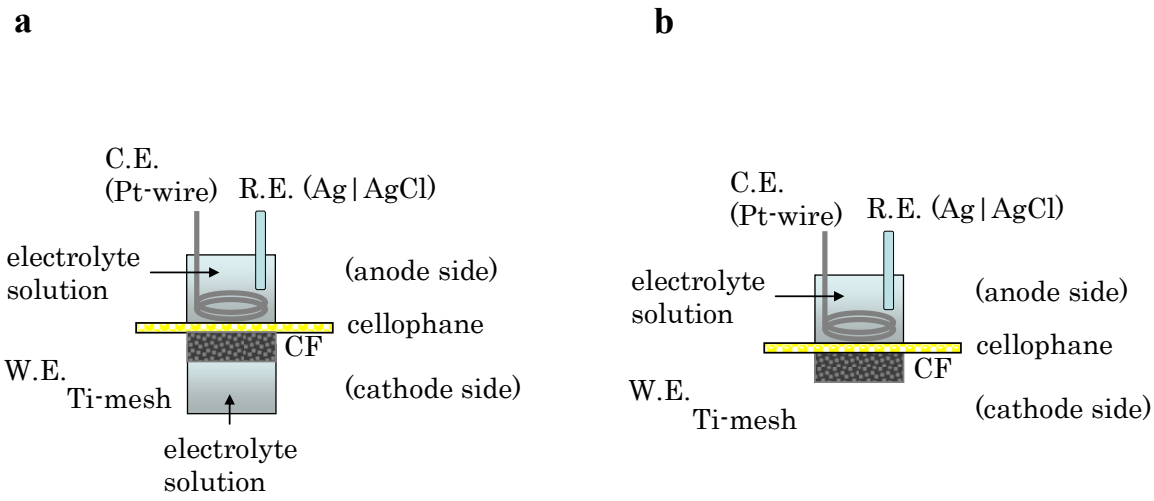


**Supplementary Figure 5** Schematic structures of electrochemical cells for CF-biocathodes in (**a**) sink-type cell (S-cell) and (**b**) open-air type cell (OA-cell). The solution volume of cell (**a**) is 3 ml for the anode side and 2 ml for the cathode side, and that of the cell (**b**) is 3 ml for the anode side. The internal resistance of the cells exiting the cellophane between W.E. and R.E. is 1.7 $\Omega/cm^2$.

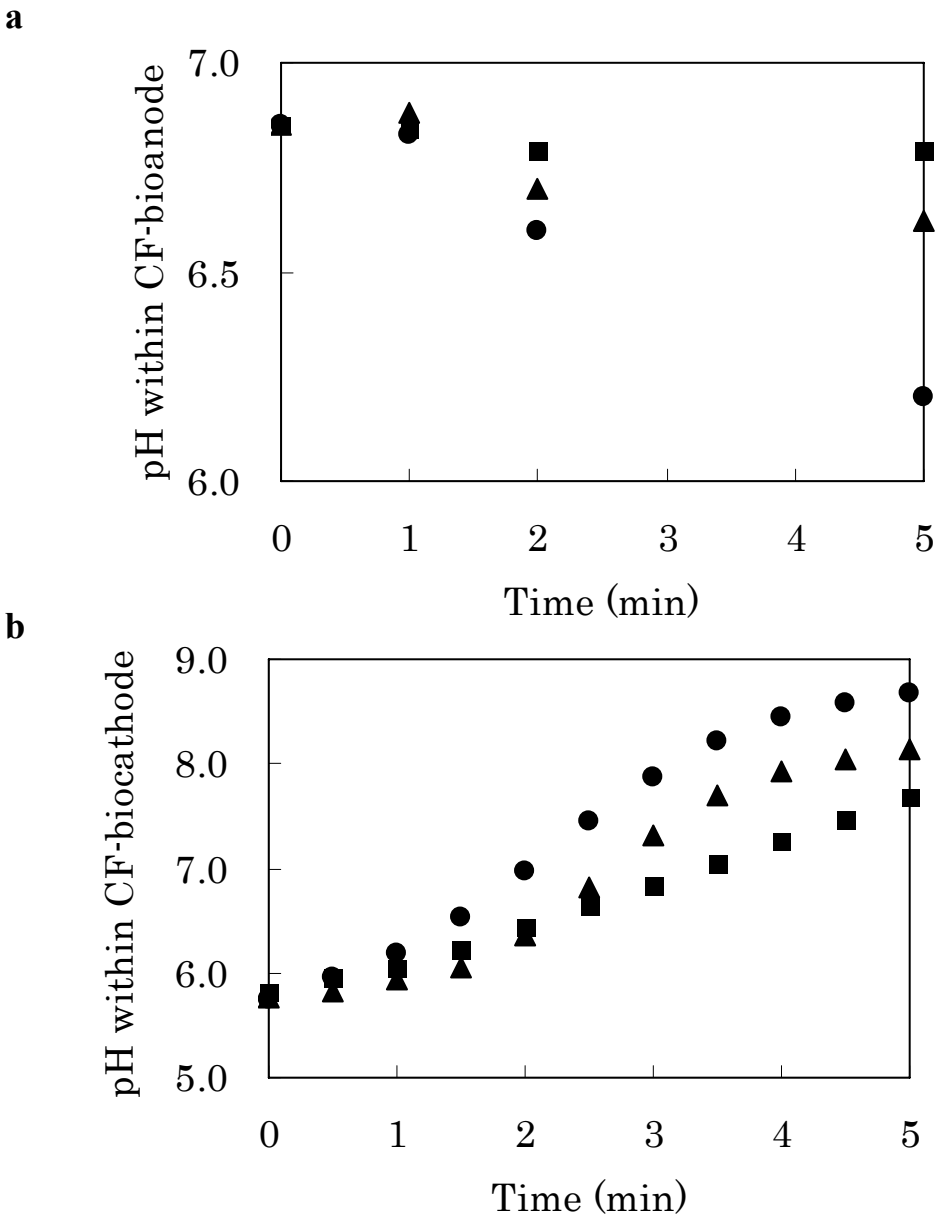


**Supplementary Figure 6** The pH change within CF-electrodes during CA in 0.1 M (●), 1.0 M (▲) and 2.0 M (■) phosphate buffer solution (pH 7.0). (**a**) CF-bioanode during CA at 0.1 V vs. Ag|AgCl in the presence of 0.4 M glucose using the electrochemical cell (**Supplementary Figure 2b**). (**b**) CF-biocathode during CA at 0 V vs. Ag|AgCl in the absence of glucose using the OA-cell (**Supplementary Figure 5b**). Slight shift of pH value from 7.0 before CA would be ascribed to the components in the immobilized layer.

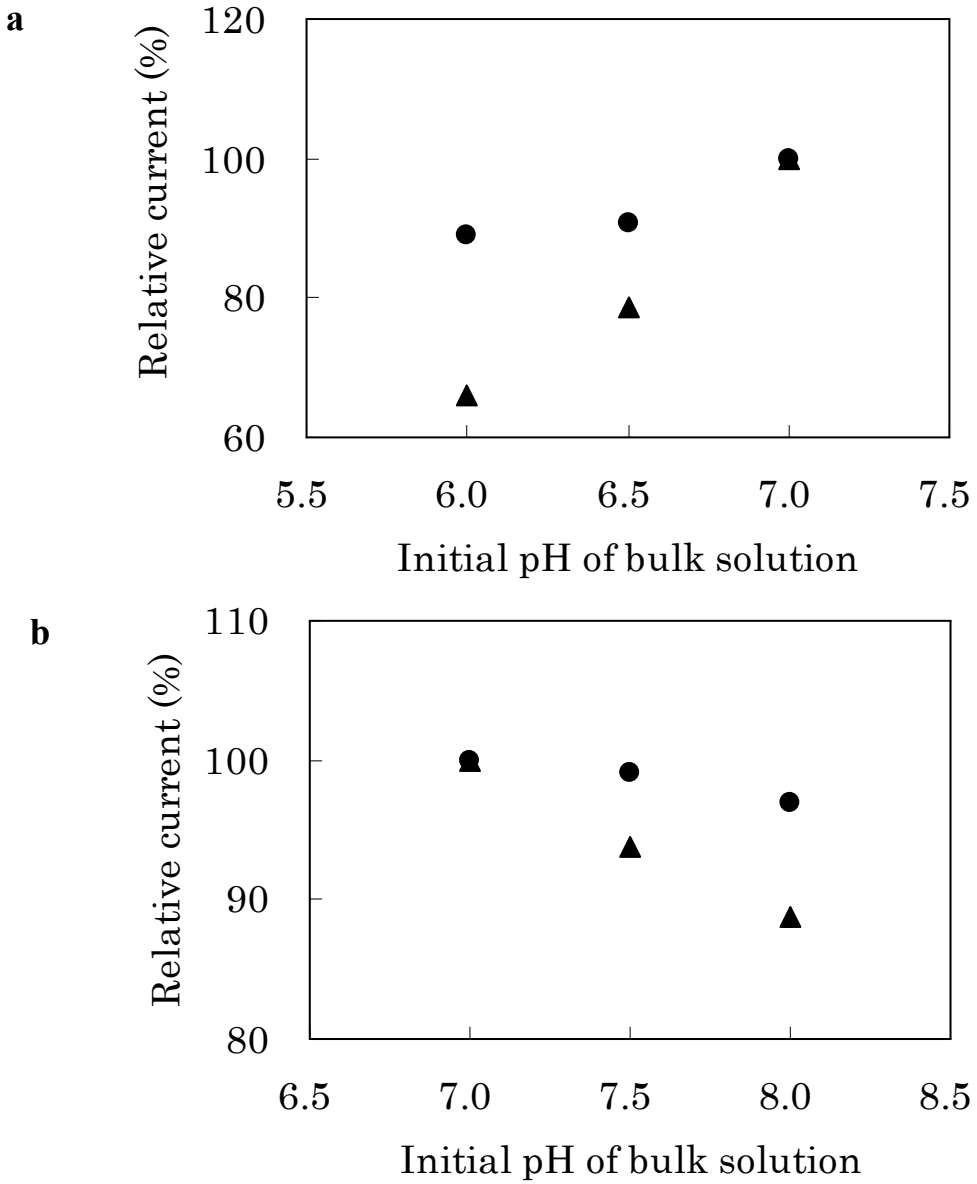


**Supplementary Figure 7** The dependence of the relative current on initial pH of the provided phosphate buffer solution. The value of current at pH 7.0 was set to 100 %. (**a**) The relative current on a CF-bioanode after 1-min (●) and 5-min (▲) CA at 0.1 V vs. Ag|AgCl in 0.1 M phosphate buffer solution (pH 6.0, 6.5 and 7.0) containing 0.4 M glucose using the electrochemical cell (**Supplementary Figure 2b**). (**b**) The relative current on a CF-biocathode after 1-min (●) and 5-min (▲) CA at 0 V vs. Ag|AgCl in 0.1 M phosphate buffer solution (pH 7.0, 7.5 and 8.0) using the OA-cell (**Supplementary Figure 5b**).

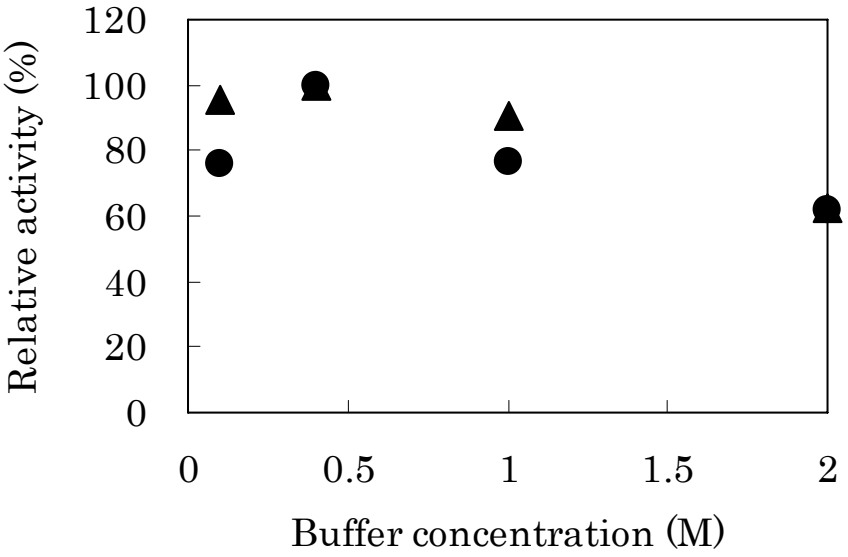


**Supplementary Figure 8** The dependence of relative enzymatic activities of GDH (●) and DI (▲) on the concentration of phosphate buffer (pH 7.0). The activities of GDH and DI at buffer concentration 0.4 M are set as 100 %, respectively.

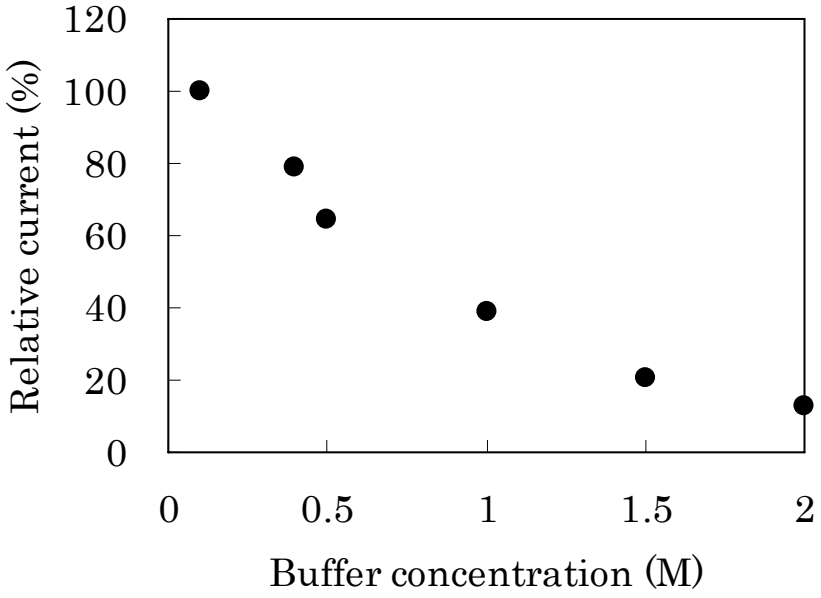


**Supplementary Figure 9** The dependence of the relative current in cathode upon the buffer concentration. A GC-electrode was used and BOD and $K_3[Fe(CN)_6]$ were dissolved in phosphate buffer solution (pH 7.0).

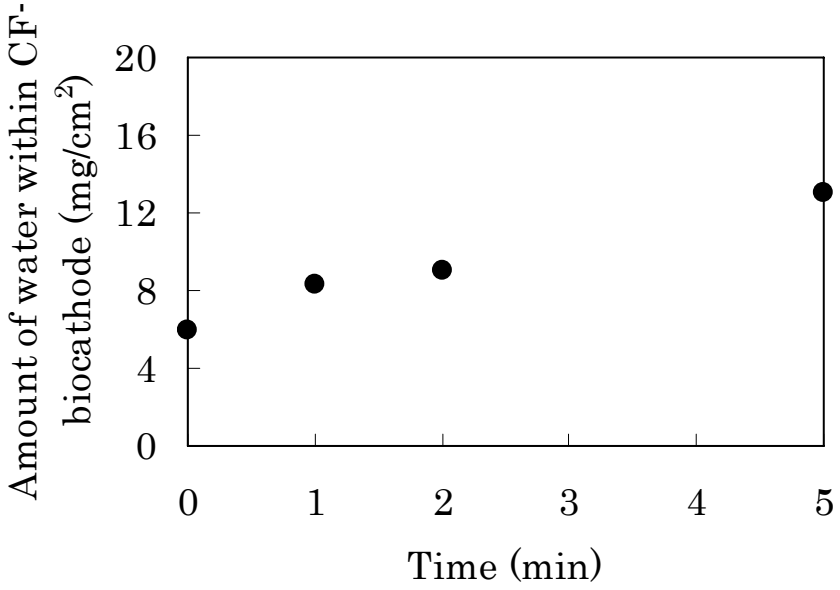


**Supplementary Figure 10** Amount of water accumulated within a CF-biocathode during CA at 0 V vs. Ag|AgCl in 1.0 M phosphate buffer solution (pH 7.0) using the OA-cell (**Supplementary Figure 5b**).

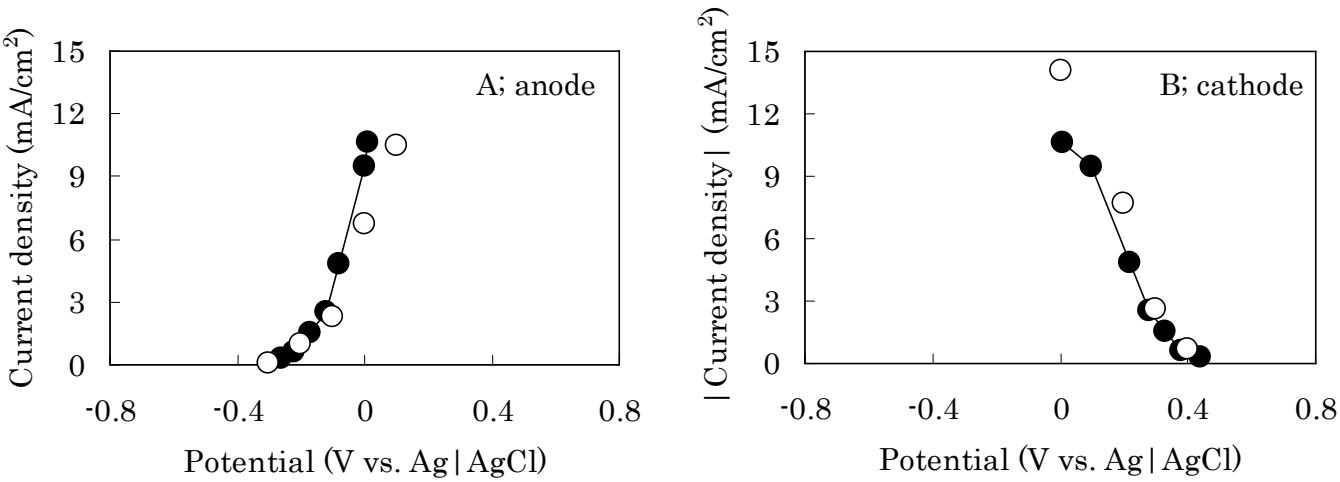


**Supplementary Figure 11** The current-potential relationship of the biofuel cell under power-generation(●) using the electrochemical cell for the biofuel cell (**Fig. 2**), compared with those of two electrochemical cells (○) using the CF-bioanode (**Supplementary Fig. 2b**) and the CF-biocathode (OA-cell, **Supplementary Fig. 5b**). All data were taken after 1-min CA in a 0.4 M glucose/1.0 M phosphate buffer solution (pH 7.0) under quiescent conditions.

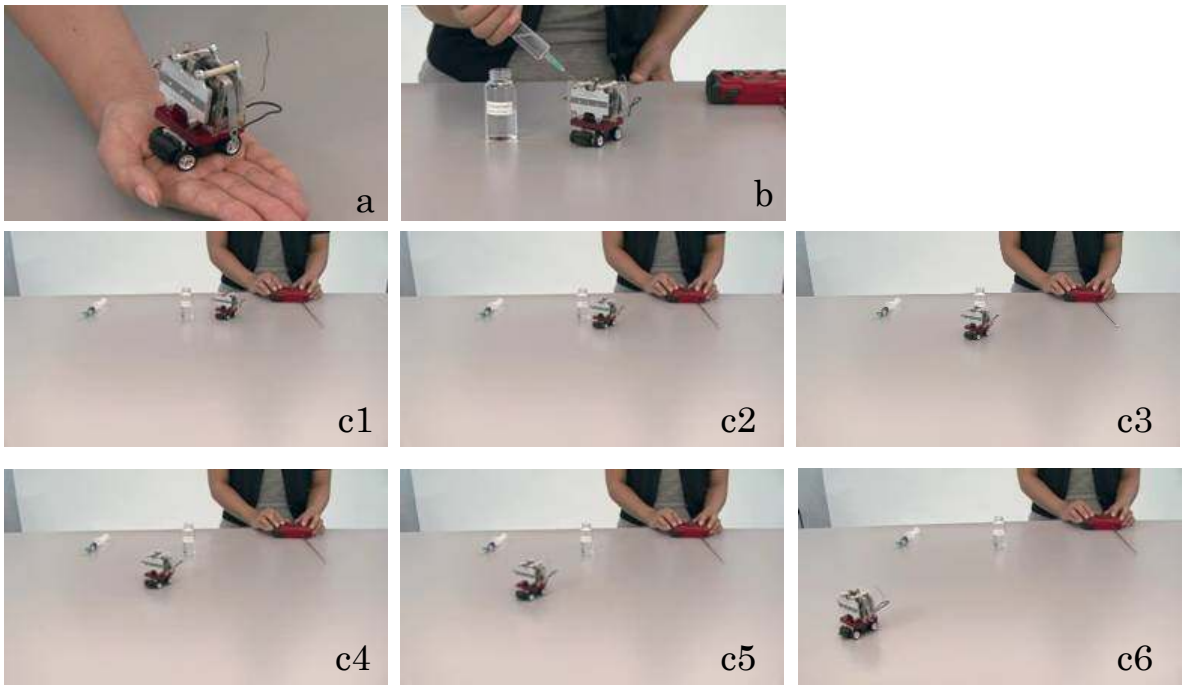


**Supplementary Figure 12** Demonstrative operation of a radio-controlled car by using the passive-type biofuel cell units (**Fig. 4**) composed of two multi-stacked biofuel cell units (**Fig. 3**). (**a**) A radio-controlled car with the biofuel cell units. (**b**) Glucose solution as fuel was injected into the cell units. (**c1-6**) Sequential photographs of the radio-controlled car in operation.

**Supplementary Website 1** Sony press release home page:
http://www.sony.net/SonyInfo/News/Press/200708/07-074E/

**Supplementary Video 1** Movie of the demonstrative operation of a radio-controlled car by using passive-type biofuel cell units (**Fig. 4**). (file; Supplementary Video-1.avi, 3 MB)